Templated fabrication of sub-100 nm periodic nanostructures

Chih-Hung Sun, Wei-Lun Min and Peng Jiang*

Received (in Cambridge, UK) 12th March 2008, Accepted 8th April 2008
First published as an Advance Article on the web 7th May 2008
DOI: 10.1039/b804182b

Periodic polymer nanoposts and metal nanohole arrays with tunable size have been fabricated by templating from spin-coated two-dimensional non close-packed colloidal crystal–polymer nanocomposites.

Subwavelength periodic metal nanohole arrays are of great scientific interest and considerable technological importance in developing miniaturized optical devices for all-optical integrated circuits (*e.g.*, optical waveguides, switches, and couplers),[1–4] information storage,[5] efficient light-emitting diodes,[6] and biosensors,[7] as well as fundamental understanding of surface plasmon enabled optical transmission and diffraction.[8] Zero-mode waveguiding through arrays of sub-100 nm nanoholes perforated in a metal film has also been demonstrated as a simple and highly parallel method for single-molecule bioanalysis at high concentrations.[9,10] Unfortunately, these important applications have been greatly impeded by the expensive and complex nanofabrication techniques (*e.g.*, electron-beam, focused ion beam, and interference lithography) in creating subwavelength nanohole arrays.[8,9,11] Attaining high-throughput and large-area fabrication continues to be a major challenge with these top-down techniques.

Bottom-up self-assembly and templating nanofabrication provide a much simpler, faster, and inexpensive alternative to nanolithography in generating periodic nanostructures.[12–15] For instance, self-assembled monolayer or multilayer colloidal crystals are used as templates to create a large variety of functional periodic nanostructures including nanohole arrays.[16–19] However, most of the available bottom-up approaches suffer from low throughput and incompatibility with mature microfabrication, limiting mass-production and on-chip integration of practical devices. Furthermore, only close-packed colloidal crystals are available through traditional self-assembly, whereas non close-packed crystals are needed to template nanohole arrays.[20–22]

We have recently developed a robust spin-coating technology that combines the simplicity and cost benefits of bottom-up colloidal self-assembly with the scalability and compatibility of standard top-down microfabrication.[23] Spin-coating enables rapid production of both 3-D and 2-D ordered colloidal crystals with remarkably large domain sizes and unusual non close-packed structures.[23,24] It also provides a scalable templating nanofabrication platform for producing a myriad of nanostructured materials, including metal nanohole arrays,[25] attolitre microvial arrays,[26] 2-D magnetic nanodots,[27] and more. Unfortunately, current spin-coating-enabled templating techniques are not flexible. The resulting nanofeature size is solely determined by the diameter of the templating silica spheres. Until now, submicrometre-scale particles (>250 nm diameter) have been demonstrated to form 2-D colloidal templates.[24] However, non close-packed crystalline arrays consisting of sub-100 nm particles have not been achieved by the spin-coating technique.

Here we report a flexible and scalable non-lithographic approach for fabricating large-area sub-100 nm periodic nanostructures using submicrometre-sized particles as templates. The resulting nanofeature size can be easily adjusted by controlling the templating conditions. Sub-100 nm patterns, whose size is only ~20% of the original templating sphere diameter, can be fabricated over an 80 cm^2 area.

Fig. 1 shows a schematic outline of the new templating procedure for making periodic metal nanohole arrays. The established spin-coating technique is utilized to create a monolayer of non close-packed silica colloidal crystals embedded in a thin layer of polymer matrix as structural templates.[23,24] In the spin-coating technique, monodisperse silica particles are dispersed in non-volatile ethoxylated trimethylolpropane triacrylate (ETPTA, Sartomer) monomers to form stable dispersions with a particle volume fraction of ~20%. The dispersions are then spin-coated on planar substrates (*e.g.*, glass and silicon wafer) using standard spin-coating equipment. Both multilayer and monolayer colloidal crystals with non close-packed structures can be formed by simply tuning the spin-coating speed and time.[23,24] The ETPTA monomers can then be polymerized by exposure to ultraviolet radiation to immobilize the shear-aligned particle arrays.

The resulting colloidal crystal–polymer nanocomposite has a thin polymer wetting layer (~100 nm thick) between the silica monolayer and the substrate.[26] The current templating

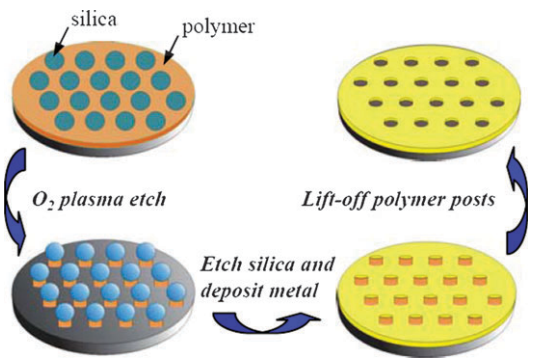

Fig. 1 Schematic illustration of the fabrication procedures for making periodic arrays of metal nanoholes with tunable size by using monolayer non close-packed colloidal crystal–polymer nanocomposites as templates

Department of Chemical Engineering, University of Florida, Gainesville, FL 32611, USA. E-mail: pjiang@che.ufl.edu; Fax: +1 352-392-9513; Tel: +1 352-392-2189

technique is aimed at utilizing this polymer wetting layer to transfer the hexagonal patterns of spin-coated colloidal monolayers consisting of submicrometre-sized particles into arrays of nanoholes with a sub-100 nm diameter (Fig. 1). In this approach, conventional oxygen plasma etching is firstly applied to partially remove the polymer matrix between the non close-packed colloidal arrays. Silica particles function as etching masks during the oxygen plasma etching process. They protect the polymer wetting layer immediately underneath them to form polymer posts whose size can be easily adjusted by controlling the etching conditions. The templating silica particles can then be removed by dissolving in a 2% hydrofluoric acid aqueous solution for 2 min. A thin layer of metal can finally be deposited between the exposed polymer posts, followed by lifting-off polymer templates to form hexagonal arrays of metal nanoholes with tunable size.

Fig. 2A–C show top-view scanning electron microscope (SEM) images of the templated polymer posts after oxygen plasma etching operating at 40 mTorr pressure, 40 sccm flow rate, and 100 W on a Unaxis Shuttlelock RIE/ICP reactive ion etcher for 2, 6, and 8 min, respectively, followed by hydrofluoric acid wash to remove the templating silica particles. It is evident that the resulting polymer posts retain the long-range hexagonal ordering and the inter-particle distance of the original non close-packed colloidal monolayer consisting of 360 nm silica spheres.[24] The cross-sections of the posts are round-shaped for all three above conditions, indicating uniform etching of ETPTA from the peripheries of the templated posts.

It is also apparent from Fig. 2A–C that longer etching duration leads to smaller polymer posts. We determine the size and size distribution of the templated posts by averaging over 100 posts using image analysis software (Scion Image). Fig. 2D shows the dependence of the size of the templated posts on the oxygen plasma etching time. The measured size

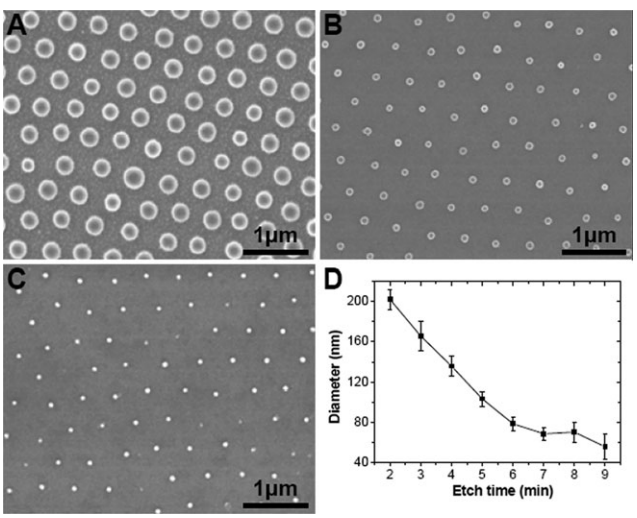

Fig. 2 Templated polymer posts with adjustable size. (A–C) SEM images of polymer posts with diameters of 202 ± 10 nm, 78 ± 7 nm, and 70 ± 10 nm after 2, 6, and 8 min oxygen plasma etching, respectively. (D) Size dependence of the templated polymer posts on the oxygen plasma etching time. 360 nm silica spheres are used as the original templates.

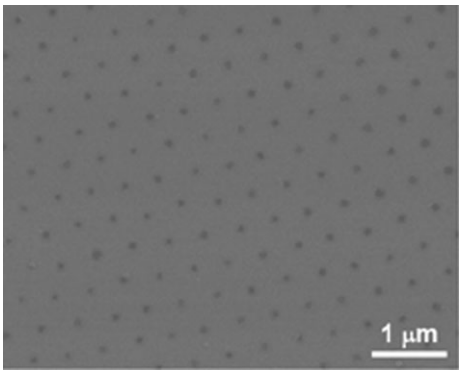

Fig. 3 SEM image of an array of gold nanoholes with 89 nm diameter templated from a monolayer nanocomposite consisting of 360 nm silica spheres.

standard deviation is around 10%, which is a little bit worse than that of the templating silica spheres (~5–7%). Importantly, much smaller polymer posts (as small as 55 nm) than the original templating silica spheres (360 nm) can be achieved. This represents ~85% shrinkage of the template size. When longer plasma etching duration (>9 min) is applied, the polymer posts become too narrow to support the silica particles, resulting in the collapse of the particles and subsequent complete etching of the polymer posts.

After removing the silica particles by hydrofluoric acid wash, the polymer posts can be used as sacrificial deposition masks to template metal nanohole arrays with tunable size. A thin layer of metal is deposited by traditional physical vapor deposition techniques (*e.g.*, electron-beam evaporation and sputtering) to fill up the spacing between the non close-packed polymer posts. As the adhesion between the polymer and the substrate is quite low, the posts can be easily removed by a gentle sweeping using a cleanroom Q-tip under flowing water, resulting in the formation of wafer-scale periodic nanohole arrays. Fig. 3 shows a SEM image of a templated gold nanohole array with 89 ± 13 nm diameter. The nanoholes keep the same long-range hexagonal ordering and inter-particle distance as the original monolayer colloidal crystal template.[24] The optical transmission properties of the templated metallic nanohole arrays with tunable structural parameters are still under investigation and will be reported in a future publication.

Besides providing a much simpler approach than nanolithography for generating sub-100 nm nanohole arrays, the new templating nanofabrication approach enables creation of complex micropatterns that are not easily available by traditional top-down techniques. Fig. 4A and 4B show top- and side-view SEM images of arrays of "micro-candles" templated from spin-coated colloidal monolayers. In this approach, non close-packed silica particles are firstly used as etching masks during oxygen plasma etching to pattern polymer posts underneath them as described above. The released silica spheres can then be utilized as etching masks for the second time during chlorine reactive ion etching (RIE, 5 mTorr pressure, 20 SCCM chlorine flow rate, and 80 W) to generate ordered arrays of silicon pillars.[28] The polymer posts are not affected by the chlorine RIE process, forming "candle wicks" on top of the templated silicon pillars after removing the templating silica particles by a brief hydrofluoric acid wash.

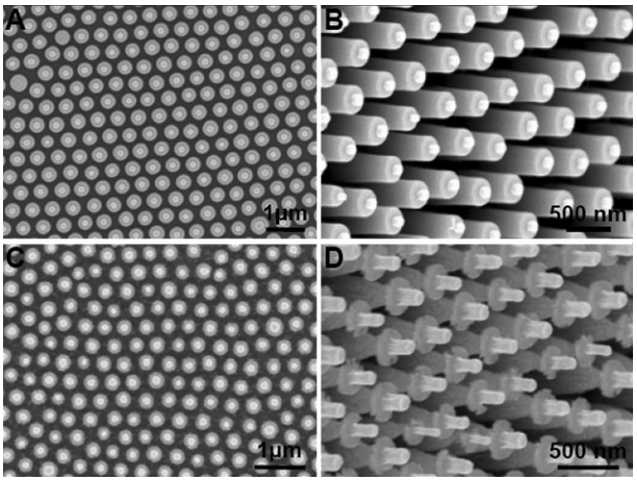

Fig. 4 (A and B) Top- and side-view SEM images of an array of silicon "micro-candles" templated from a spin-coated 2-D colloidal crystal. (C and D) Top- and side-view SEM images of a templated array of GaSb "micro-candle stands".

The height of the polymer posts can also affect the spatial distribution of the reactive ions during the above particle-masked RIE process, resulting in the formation of unusual "candle-stand shaped" micropatterns in a gallium antimonide (GaSb) substrate as shown in Fig. 4C and 4D. Due to different substrate wettabilities, the polymer wetting layer on a GaSb wafer ($\sim$500 nm thick) is much thicker than that on a silicon or a glass substrate ($\sim$100 nm). The shadowing effect created by the templating silica spheres is then significantly affected by the different polymer spacer height. On a silicon wafer, the templating silica particles are close to the substrate surface, resulting in effective shadowing of the regions underneath the particles. This leads to the formation of pillars with vertical sidewalls and almost the same diameter as that of silica spheres. While for a GaSb substrate under similar chlorine RIE conditions, the tall polymer posts between the substrate and the templating particles change the spatial distribution of the reactive chlorine ions, leading to the formation of tapered pillars with flat circular caps (Fig. 4D). The cap size is similar to that of the templating silica spheres. GaSb pillars with a high aspect ratio and vertical sidewalls resembling the silicon pillars as shown in Fig. 4B have previously been fabricated using lithographically patterned photoresist as an etching mask under similar chlorine RIE conditions as described above.[29] This verifies the importance of the polymer posts in controlling the shape of the templated microstructures during the particle-masked dry etching process.

In summary, we have developed a simple yet scalable templating nanofabrication technqiue that enables the creation of periodic nanostructures with tunable feature size. Sub-100 nm metal nanohole arrays, which have important technological applications in integrated nanophotonics and bio-microanalysis, can be easily templated over a large area. The polymer wetting layer between the spin-coated colloidal monolayer and the substrate also plays a crucial role in determining the shape of the templated microstructures that have broad applications ranging from plasmonics[30] to broad-band antireflection coatings for solar cells.[28]

This work is supported in part by the NSF under Grant No. CBET-0651780 and CBET-0744879, start-up funds from the University of Florida, and the UF Research Opportunity Incentive Seed Fund.

Notes and references

1. W. L. Barnes, A. Dereux and T. W. Ebbesen, *Nature*, 2003, **424**, 824–830.
2. E. Hutter and J. H. Fendler, *Adv. Mater.*, 2004, **16**, 1685.
3. E. Altewischer, M. P. van Exter and J. P. Woerdman, *Nature*, 2002, **418**, 304–306.
4. P. Andrew and W. L. Barnes, *Science*, 2004, **306**, 1002–1005.
5. D. Jenkins, W. Clegg, J. Windmill, S. Edmund, P. Davey, D. Newman, C. D. Wright, M. Loze, M. Armand, R. Atkinson, B. Hendren and P. Nutter, *Microsyst. Technol.*, 2003, **10**, 66–75.
6. K. Okamoto, I. Niki, A. Shvartser, Y. Narukawa, T. Mukai and A. Scherer, *Nat. Mater.*, 2004, **3**, 601–605.
7. A. Lesuffleur, H. Im, N. C. Lindquist and S. H. Oh, *Appl. Phys. Lett.*, 2007, **90**, 243110.
8. T. W. Ebbesen, H. J. Lezec, H. F. Ghaemi, T. Thio and P. A. Wolff, *Nature*, 1998, **391**, 667–669.
9. M. J. Levene, J. Korlach, S. W. Turner, M. Foquet, H. G. Craighead and W. W. Webb, *Science*, 2003, **299**, 682–686.
10. C. Genet and T. W. Ebbesen, *Nature*, 2007, **445**, 39–46.
11. J. Henzie, M. H. Lee and T. W. Odom, *Nat. Nanotechnol.*, 2007, **2**, 549–554.
12. D. G. Choi, H. K. Yu, S. G. Jang and S. M. Yang, *J. Am. Chem. Soc.*, 2004, **126**, 7019–7025.
13. G. A. Ozin and A. C. Arsenault, *Nanochemistry: A Chemical Approach to Nanomaterials,* RSC Publishing, Cambridge, 2005.
14. Y. N. Xia, B. Gates, Y. D. Yin and Y. Lu, *Adv. Mater.*, 2000, **12**, 693–713.
15. Y. A. Vlasov, X. Z. Bo, J. C. Sturm and D. J. Norris, *Nature*, 2001, **414**, 289–293.
16. J. C. Hulteen and R. P. Van Duyne, *J. Vac. Sci. Technol., A*, 1995, **13**, 1553–1558.
17. A. Kosiorek, W. Kandulski, P. Chudzinski, K. Kempa and M. Giersig, *Nano Lett.*, 2004, **4**, 1359–1363.
18. P. M. Tessier, O. D. Velev, A. T. Kalambur, J. F. Rabolt, A. M. Lenhoff and E. W. Kaler, *J. Am. Chem. Soc.*, 2000, **122**, 9554–9555.
19. R. M. Cole, J. J. Baumberg, F. J. Garcia de Abajo, S. Mahajan, M. Abdelsalam and P. N. Bartlett, *Nano Lett.*, 2007, **7**, 2094–2100.
20. S. G. Jang, H. K. Yu, D. G. Choi and S. M. Yang, *Chem. Mater.*, 2006, **18**, 6103–6105.
21. S. O. Lumsdon, E. W. Kaler, J. P. William and O. D. Velev, *Appl. Phys. Lett.*, 2003, **82**, 949–951.
22. M. E. Abdelsalam, P. N. Bartlett, J. J. Baumberg and S. Coyle, *Adv. Mater.*, 2004, **16**, 90–93.
23. P. Jiang and M. J. McFarland, *J. Am. Chem. Soc.*, 2004, **126**, 13778–13786.
24. P. Jiang, T. Prasad, M. J. McFarland and V. L. Colvin, *Appl. Phys. Lett.*, 2006, **89**, 011908.
25. P. Jiang and M. J. McFarland, *J. Am. Chem. Soc.*, 2005, **127**, 3710–3711.
26. P. Jiang, *Chem. Commun.*, 2005, 1699–1701.
27. P. Jiang, *Langmuir*, 2006, **22**, 3955–3958.
28. C. H. Sun, P. Jiang and B. Jiang, *Appl. Phys. Lett.*, 2008, 061112.
29. Y. Kanamori, K. Kobayashi, H. Yugami and K. Hane, *Jpn. J. Appl. Phys., Part 1*, 2003, **42**, 4020–4023.
30. S. Wang, D. F. P. Pile, C. Sun and X. Zhang, *Nano Lett.*, 2007, **7**, 1076–1080.